A Family of Aligned C-Curved Nanoarches

Da Deng and Jim Yang Lee*

Department of Chemical & Biomolecular Engineering, Faculty of Engineering, National University of Singapore, 10 Kent Ridge Crescent, Singapore 119260

ARTICLE

ABSTRACT One-dimensional (1-D) nanomaterials are basic building blocks for the construction of nanoscale devices. However, the fabrication and alignment of 1-D nanomaterials with specific geometry and composition on a given substrate is a significant challenge. Herein we show a successful example of fabricating a family of aligned 1-D C-curved nanoarches of different compositions on an extended Si surface by a simple and scalable method. The nanoarches are made up of either single-crystalline Sn nanorods encapsulated in carbon nanotubes (CNTs), SnO_2 nanotubes, or CNTs. The aligned 1-D C-curved nanoarches of single-crystalline Sn nanorods in CNTs are prepared first by a facile *in situ* reduction of SnO_2 nanoparticles under standard chemical vapor deposition conditions. Nanoarches of CNTs and SnO_2 nanotubes were then derived from the Sn@CNT nanoarches by acid etching and by calcination in air, respectively.

KEYWORDS: carbon nanotube · Sn@CNT · SnO_2 nanotube · C-curved nanoarch

The discovery of CNTs has stimulated strong interest in other 1-D nanomaterials, including those of metals, metal oxides, semiconductors, and their composites.[1−13] These 1-D nanomaterials possess unique properties that can be explored for technological advances in optoelectronics,[4] energy storage,[10] sensor development,[11] catalysis,[12] and surface modification.[8,9,13] While the extensively studied CNTs can now be fabricated as single-wall and multiwall variants or in other more complex 1-D morphologies,[7,14−17] the synthesis of other non-carbon-based 1-D nanomaterials is still in infancy. There is also increasing interest in synthesizing nanocomposites of CNTs and metals or metal oxides to take advantage of the benefits of combined material properties.[3,18] Among the non-carbon 1-D nanomaterials, metal oxide nanotubes have drawn the most attention.[19] These metal oxide nanotubes are generally produced by laborious template-assisted methods. Most of the nanotubes produced are straight because of the limited variety of template geometry. In addition, there is also difficulty in aligning the nanotubes on the growth surface.

Aligning 1-D nanomaterials with the desired curvature and composition into well-ordered, oriented nanostructures on a surface can be a design requirement for advanced applications, such as fabrication of nanodevices.[13,16,20,21] At the *micro level*, the integration of 1-D nanomaterials into devices must allow the special properties of individual 1-D nanomaterial to be easily accessible to deliver efficiency and performance in applications.[20] An appropriately aligned nanostructure may also generate interesting properties at the *macro level*, such as roughness-enhanced superhydrophobicity of the lotus leaf and gecko foot surfaces.[8,9,13,22] The alignment of 1-D nanomaterials is currently limited to nanostructures with one end attached to the substrate and the other end free-standing.[8,9,16] There is no report on the fabrication of aligned 1-D nanomaterials with curvature where both ends are affixed to the substrate. The arch-like architecture may provide new opportunities for application exploration.

We report here, for the first time, the fabrication of a family of aligned 1-D C-curved nanoarches of (1) single-crystalline Sn nanorods encapsulated in CNTs (a potential superconductor[3]), (2) carbon nanotubes (a conductor[23]), and (3) SnO_2 nanotubes (a semiconductor) on Si wafers by a simple and scalable method. Here the term "aligned" is used to refer to some apparent order in the orientation and distribution of the C-curved nanoarches on the Si wafer surface.[24,25] These aligned 1-D nanomaterials may be used to provide elasticity and three-dimensional connectivity at the micro level or as the template for the fabrication of aligned nanoarches of other materials. At the macro level, the ordered assembly of aligned 1-D C-curved nanoarches

*Address correspondence to cheleejy@nus.edu.sg.

Received for review March 20, 2009 and accepted June 15, 2009.

Published online June 23, 2009.
10.1021/nn900279b CCC: $40.75

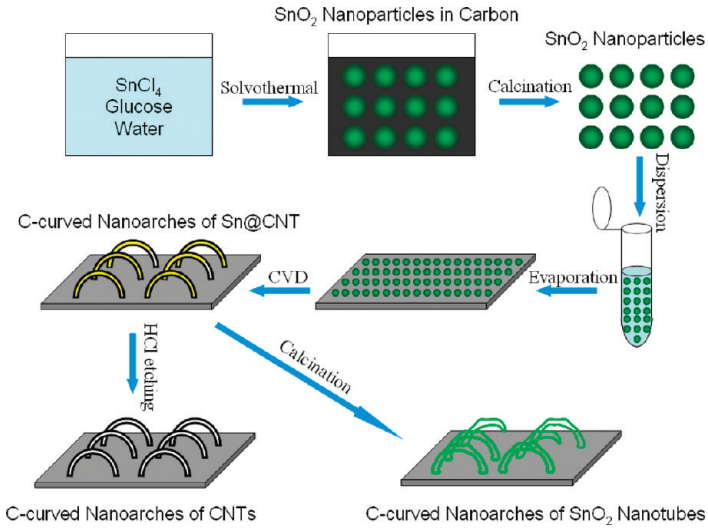

Figure 1. Schematic of experimental procedures showing the changes in morphology and material composition in each step.

over an extended surface can lead to substantial modification of the surface properties of the substrate, for example, the wettability of Si wafer, which depends strongly on the chemical and topographical properties of the surface.[13,22] Figure 1 is the process flow of the preparation method.

Aligned 1-D C-Curved Nanoarches of CNT with Encapsulated Crystalline Sn Nanorods. The FESEM images of aligned 1-D Sn in CNT (Sn@C) C-curved nanoarches on Si wafer are shown in Figure 2a−c at different magnifications and in different perspectives. The low magnification FESEM top view (Figure 2a) shows the proliferation and nearly uniform coverage of the nanoarches on the Si surface, at a density of about $\sim 6.2 \times 10^{11}/m^2$. The low magnification FESEM side views (insets of Figure 2a and Figure 2b) demonstrate most vividly the semicircular 1-D arch-like architecture: each nanotube is bent with its two ends affixed to the wafer surface forming an arch-like turned letter C with a height of ~500 nm and a width of ~500 nm. In the side view of a few aligned 1-D C-curved nanoarches (Figure 2c), the difference in contrast between the core and surface regions of the nanoarches confirms the coaxial *rod-in-tube* heterostructure. It also shows that the two ends of the nanotubes are solidly attached to the Si surface. It was found that 20 min of ultrasonication in hexane for the TEM sample preparation would not dislodge the aligned C-curved composite nanostructure from the wafer. The rod-in-tube nanostructure is more clearly shown in the TEM image of Figure 2d. The inset of Figure 2d also shows a C-curved CNT nanoarch with a partially filled metallic Sn interior. The symmetric diffraction spots in the SAED pattern of the nanoarches (inset of Figure 2d) could all be indexed to single-crystalline Sn, and hence the Sn nanorod core is single-crystalline. The weak diffraction rings could be attributed to the $\{002\}_C$ planes of the polycrystalline CNT shell. The nanocomposite structure was further confirmed by HRTEM lattice imaging (Figure 2e). The measured fringe spacing of the dark core is 0.29 nm and agrees well with the $\{200\}_{Sn}$ set of planes, corroborating that the metallic Sn nanorod is inside the CNT and single-crystalline. The lighter color carbon shell is about 8 nm thick, and the measured fringe spacing of 0.35 nm (corresponding to the $\{002\}_C$ *d* spacing) also verifies the formation of a CNT shell. The lack of extended graphene sheets in the CNTs, the curvature in the graphene sheets, and the slightly expanded $\{002\}_C$ *d* spacing (0.34 nm for graphite) suggest a low degree of graphitization. For low-graphitized CNTs, there should be significant defects with a large number of pentagonal and heptagonal rings besides the usual hexagonal rings in the carbon nanostructure.[14] The nanoarches were also analyzed by Sn3d XPS (Figure 2f). Compared to the precursor SnO_2 nanoparticles (SI1d in Supporting Information), the strong and distinctively sharp Sn^0 peaks indicate the reduction of SnO_2 to metallic Sn. The reduction was, however, incomplete, as can be seen from the remnant presence of oxidized Sn in the XPS spectrum. XPS analysis also confirmed the presence of carbon nanotubes with sp^2 C═C and sp^3 C−C bonds (SI2 in Supporting Information).

The formation of these unique aligned C-curved Sn@C nanoarches could be rationalized as follows: Under the experimental conditions, SnO_2 nanoparticles were converted to metallic Sn by the reducing action of acetylene.[3] As metallic Sn has a low melting point (232 °C) and a high boiling point (2270 °C), liquid Sn droplets were formed on the Si surface at the reaction temperature of 650 °C. The Sn droplets are catalytic to carbon deposition from C_2H_2 decomposition.[2] The carbon deposit would dissolve into Sn initially. However, the solubility of carbon in Sn is limited, and carbon in excess of its solubility limit in Sn would emerge from the surface and start to bud into a tubular structure (due to the intrinsic anisotropic character of carbon).[3] The continuous supply of carbon sustained the CNT growth. The growth was propagated by the formation and concomitant insertion of pentagonal and heptagonal rings in addition to the hexagonal rings. The addition of carbon with different ring structures to the graphene sheets would result in curvature in the growing nanostructure as an attempt to lower the energy of the structure.[7] Along with the growth of CNTs, capillary forces would draw molten Sn on the Si surface into the nanotubes, filling their interior to different degrees. The Sn-filled CNT with the additional weight load introduced by metallic Sn could vacillate in a flowing gas. Once the free end of the CNT made a second contact with the wafer surface and adsorbed there, a complete C-curved nanoarch was formed. The different growth stages discussed above could be detected experimentally as shown in SI3b of Supporting Information. In addition, when a group of CNTs grew in close proximity, they could form an extended bridge struc-

ture strong enough to uphold a C/SnO_x aggregate (SI3a of Supporting Information). (The C/SnO_x aggregate was the result of incomplete reduction of SnO_2 nanoparticles aggregated on the silicon wafer.)

As an example of one of the potential applications at the macro level, the wettability of the Si wafer modified by aligned 1-D C-curved nanoarches of CNTs with single-crystalline Sn nanorod cores was measured. Compared to the untreated Si wafer (Figure 2h), Si wettability underwent substantial changes from hydrophilic (contact angle of ~71°) to superhydrophobic (contact angle of ~151°) after the deposition of nanoarches (Figure 2g). The increase in hydrophobicity was caused by the ordered roughness and enhanced by the entrapment of air underneath the C-curved nanoarches. For a macroscopic water droplet on the modified wafer, the nanoarches provide numerous nanoscale air bubbles under it and reduce the contact of the water droplet with the Si wafer. As air is completely hydrophobic (180°), surface-roughness-induced entrapment of air could lead to superhydrophobicity. The phenomenon could also be understood in terms of the Cassie−Baxter equation ($\cos\theta_{rough} = f_1 \cos\theta - f_2$, where θ_{rough} and θ are the contact angles of the rough and flat surfaces, respectively; f_1 is the fraction of the solid/water interface, and f_2 is the fraction of the air/water interface, $f_1 + f_2 = 1$). A rough surface introduces more air entrapment; f_2 would increase, and a larger contact angle (*i.e.*, hydrophobicity) results.[26] In all of the reported superhydrophobic surfaces of 1-D nanostructured materials, air is trapped in the space between neighboring solid nanostructures.[8,9,13] In the current case, however, there is also an air pocket below the arch-like nanoarchitecture. The situation may be likened to a nanoumbrella with microscopic air bubbles underneath the shade cover. This is a new mode of wettability modification that has not been observed before and warrants further investigations.[22]

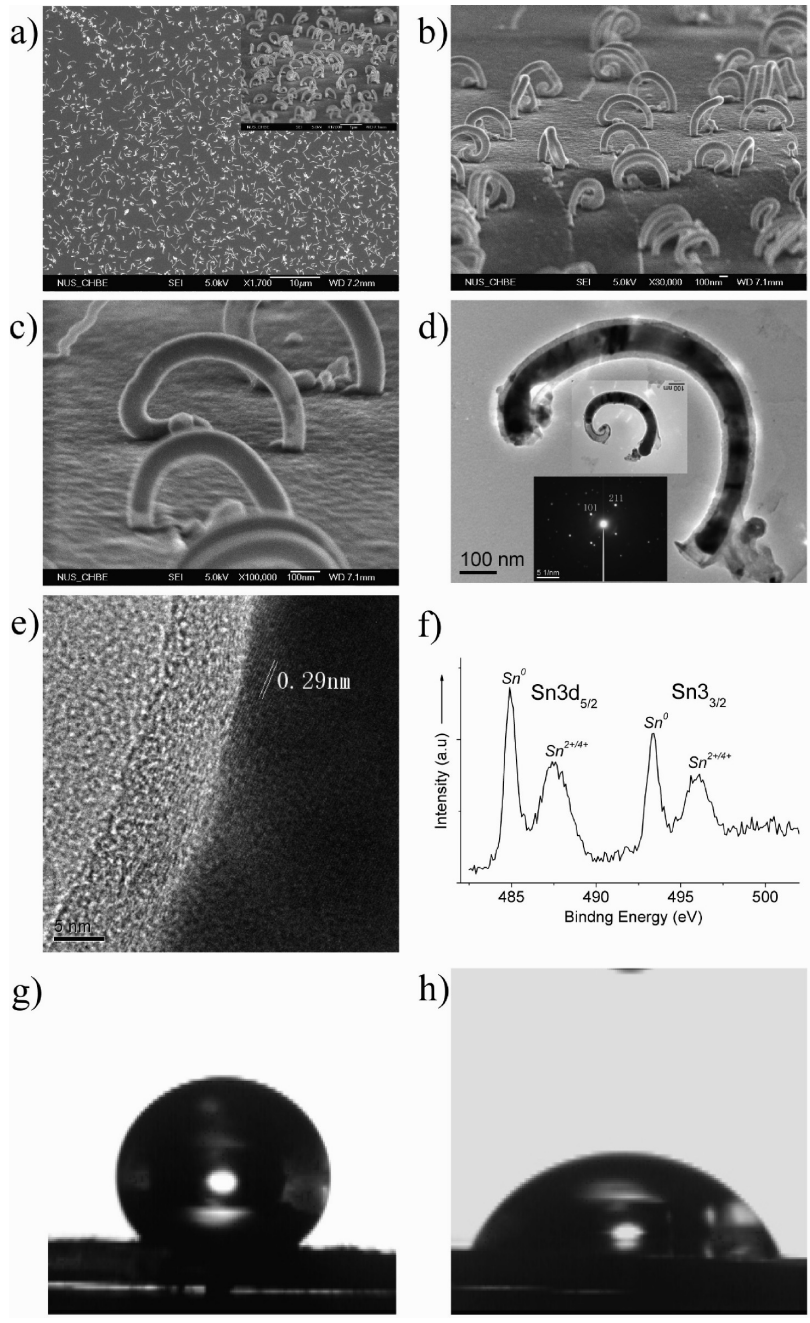

Figure 2. Aligned 1-D C-curved nanoarches of CNT encapsulating crystalline tin nanorods. FESEM images at low magnification top view (a) and side view (inset of a). High magnification side views (b,c). TEM images (d, and the inset in d) and SAED pattern (inset in d). HRTEM image of the side of a C-curved carbon nanotube encapsulating crystalline tin nanorod (e). XPS Sn3d spectrum (f). Optical image of a water droplet on the Si wafer with surface modification by C-curved CNT encapsulating crystalline tin nanorods (g) and Si wafer without any surface modification (h).

Aligned 1-D C-Curved Nanoarches of SnO_2 Nanotubes. The aligned 1-D C-curved Sn@C nanoarches could be used to derive aligned 1-D C-curved nanoarches of SnO_2 nanotubes and CNTs easily (Figure 1). Aligned 1-D C-curved nanoarches of SnO_2 nanotubes were obtained from the Sn@CNT precursor by calcination in air. The low magnification FESEM image (Figure 3a) shows the conservation of precursor geometry, without much change in the uniformity and surface density of nanoarch distribution on the wafer surface. The inset of Figure 3a shows the side view of a nanoarch of the SnO_2 nanotube with two ends attached to the Si wafer surface, which was templated from an arch precursor of CNT fully filled with a metallic Sn rod. A higher magnification FESEM image (Figure 3b) shows that the nanotube surface is corrugated and the diameter is not uniform throughout. Figure 3b also shows a product templated from an arch precursor of CNT partially filled with Sn. Here, one end of the SnO_2 nanotube is at-

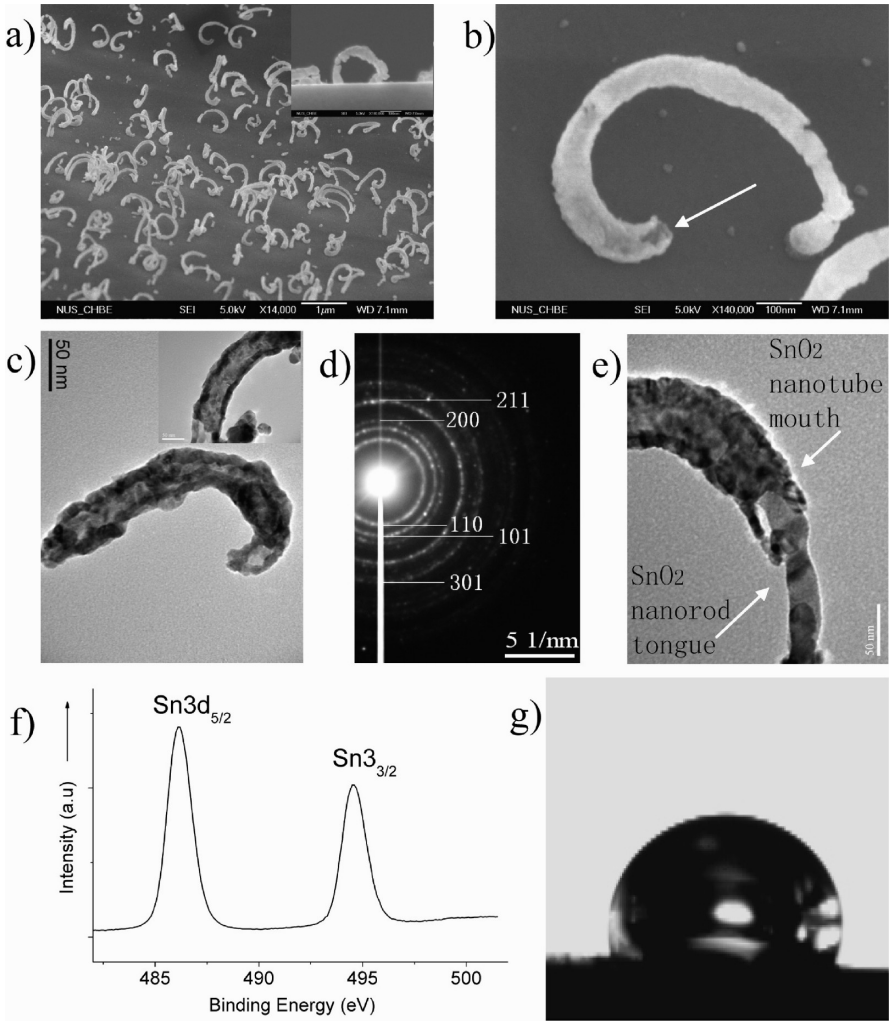

Figure 3. Aligned 1-D C-curved nanoarches of SnO_2 nanotubes. FESEM image at low magnification side view (a) and a typical nanoarch with its two ends attached to the wafer surface (inset). Another representative nanoarch of SnO_2 nanotube with the arrow showing the tubular structure (b). TEM image of a representative C-curved nanoarch of the SnO_2 nanotube (c) and a section of the nanoarch showing the tubular structure more clearly (inset). SAED pattern (d). TEM of a section of the arch-like SnO_2 nanotube showing an interesting tongue-in-mouth structure (e). XPS Sn3d spectrum (f). Optical image of a water droplet on the Si wafer with surface modification by C-curved nanoarches of SnO_2 nanotubes (g).

tached to the wafer surface, while the other end is open. The open end offers an opportunity to examine the tubular structure more closely. The formation of C-curved SnO_2 nanotubes was further confirmed by the TEM imaging (Figure 3c and inset), which showed a brighter core area throughout the curved structure and a rugged surface texture. The SAED pattern (Figure 3d) shows continuous diffraction rings that match well with polycrystalline SnO_2. The Sn3d XPS spectrum (Figure 4f) also confirmed the presence of the Sn(IV) oxidation state.

The formation of SnO_2 nanotubes (instead of SnO_2 nanorods) could be rationalized as follows: During calcination in air, the polycrystalline CNTs were oxidized at temperatures much higher than the melting point of metallic Sn (>400 °C).[27,28] Unlike the slow oxidization of pristine Sn nanoparticles to SnO_2 nanoparticles at low temperatures (225 °C), which forms only solid structures,[29] the preoxidation of the carbon shell at high temperatures in our case provided the conditions for melting Sn and the outward diffusion of molten Sn through the CNT. The diffused Sn was subsequently oxidized to SnO_2 once it was exposed to O_2, forming a tubular shell structure. During this process, CNTs played the role of an active template to promote the formation of SnO_2 nanotubes. Indeed, in some cases after the removal of the carbon shell when there was still molten Sn inside the SnO_2 nanotube, the molten tin would flow to the open end of the tube and was oxidized there to SnO_2, forming a tongue-in-mouth nanorod-in-nanotube structure (Figure 3e). In general, this *in situ* oxidization method for the fabrication of SnO_2 nanotubes should also be applicable to forming oxide nanotubes of other low melting point metals and alloys (*e.g.*, Pb, SnPb). While SnO_2 is generally considered as hydrophilic, the assembly of SnO_2 with the unique aligned C-curved geometry still imparted strongly hydrophobic character to the Si surface. The measured contact angle was 123° (Figure 3f). This implies that wettability in this case is strongly influenced by surface roughness or large f_2.

Aligned 1-D C-Curved Nanoarches of Carbon Nanotubes. Aligned 1-D C-curved nanoarches of CNTs were obtained from the Sn@CNT precursor by acid etching. The ease at which the nanoarches could be hollowed by treatment in dilute acid also confirms the core−shell structure and the presence of an acid-etchable core of metallic Sn. The low magnification FESEM images (Figure 4a) show that the aligned 1-D C-curved CNT nanoarches are again morphologically identical to their Sn@CNT precursor. Contrary to the Sn@CNT precursor, there is no more darkened core to contrast with the shell area because of the removal of the electron dense Sn interior (Figure 4b). This is confirmed by the TEM image of Figure 4d, which shows a translucent shell with trace Sn nanoparticles on the inside of the shell. The nanoarches prepared here are noticeably different from the arched carbon fibers reported in a previous publication,[21] which are orders of magnitude larger (1−10 μm in diameter and hundreds of micrometers in length), less ordered, and more U-shaped than C-curved. The wettability of the Si wafer decorated with C-curved CNTs was also

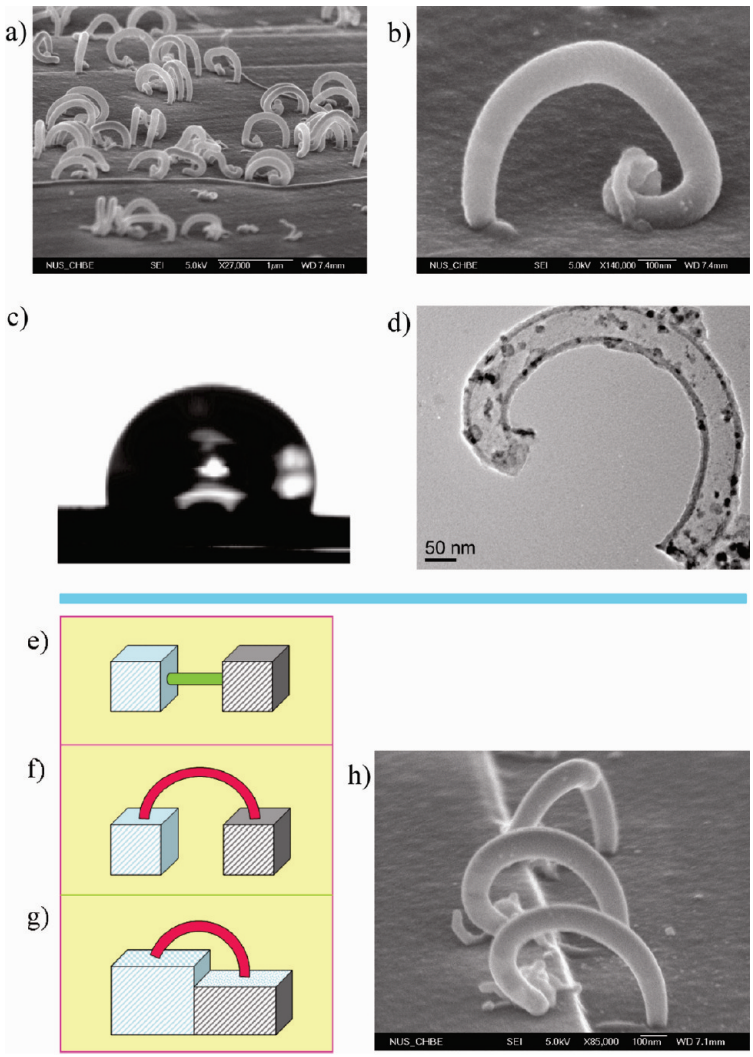

Figure 4. Aligned 1-D C-curved nanoarches of CNTs. FESEM images of side views at low (a) and high (b) magnifications. TEM image of a representative C-curved CNT nanoarch (d). Optical image of a water droplet on the Si wafer surface modified by C-curved CNT nanoarches (c). Conceptual sketches showing the ability of C-curved nanoarches to form 3-D and elastic connections (f,g) which may be preferred over a straight connection (e) in some cases. FESEM image of a few 1-D C-curved nanoarches of CNT encapsulating crystalline tin nanorods across a step in the wafer substrate (h).

measured (Figure 4c). A contact angle of about 115° was obtained. The contact angle change despite the conservation of the arch-like geometry could be the result of the acid treatment which rendered the nanoarches more hydrophilic through the introduction of surface C−O and C−H groups. The hydrophilicity of these groups negates the nanoscale roughness effect to some extent, resulting in the decrease in superhydrophobicity.

Although not studied here, this family of unique aligned 1-D C-curved nanoarches of Sn@CNTs, CNTs, or SnO_2 nanotubes on a Si wafer may also generate useful integrative properties for applications at the micro level. It is anticipated that, in the design of nanodevices, there may be a need to align 1-D nanostructures of the desired curvature and composition on a substrate to provide efficient transport of electrons or for optical and thermal excitations.[7,18−20,23] This study demonstrates one example of the enabling methodology. The family of C-curved nanoarches shown here can also provide 3-D connectivity, which may be more advantageous than linear 1-D connectivity in certain cases (see the conceptual drawings in Figure 4e *vs* panels f and g and experimentally observed 3-D connectivity in Figure 4h). Such 3-D connections may eventually find applications in the construction of nanoscale sensors, transducers, and transponders.

CONCLUSION

In summary, we have successfully fabricated a family of aligned one-dimensional C-curved nanoarches of different compositions on Si surfaces by a simple and scalable method for the first time. The nanoarches are actually nanotubes with their extremities firmly attached to the Si surface, thereby forming a turned letter C. We have also developed a new methodology for synthesizing SnO_2 nanotubes using *in situ* formed CNTs as the active template. A mechanism of formation was proposed, and the use of these nanoarches to modify Si surface wettability was investigated. The fabrication method is generic and could, in principle, be applied to the preparation of other aligned 1-D nanomaterials.

METHODS

Preparation of SnO_2 Nanoparticles. The SnO_2 nanoparticle precursor was prepared according to our previous procedure.[30] In a typical experiment, 4 mmol $SnCl_4$ and 10 mmol D-glucose monohydrate were dissolved in 35 mL of pure water. The clear mixture was transferred to a Teflon-lined autoclave and heated at 180 °C for 24 h to form SnO_2 nanoparticles dispersed in amorphous carbon. The SnO_2 nanoparticles were recovered by calcination in air to burn off the carbon. The full characterization of the SnO_2 nanoparticle precursor is in section I of the Supporting Information.

Preparation of Aligned 1-D C-Curved Nanoarches of CNT Encapsulating Crystalline Sn Nanorods. The SnO_2 nanoparticles were ultrasonically dispersed in acetone. The dispersion was dispensed onto a silicon wafer surface, and acetone was removed by evaporation.

The SnO_2 nanoparticle loaded wafer was placed inside a tubular furnace for chemical vapor deposition (CVD) of CNTs. The CVD conditions were 650 °C using a mixture of 10% C_2H_2 in N_2 at 200 sccm for 3 h. The wafer was cooled to room temperature in flowing N_2 after the reaction.

Preparation of Aligned 1-D C-Curved Nanoarches of SnO_2 Nanotubes. The aligned 1-D C-curved Sn@CNT nanoarches were calcined in air at 550 °C to completely remove the CNT shells and at the same time oxidized *in situ* the molten metallic Sn cores to SnO_2 nanotubes.

Preparation of Aligned 1-D C-Curved Nanoarches of Carbon Nanotubes. In this case, the aligned 1-D C-curved Sn@CNT nanoarches on the wafer were treated in 2 M HCl acid to etch away the metallic Sn core overnight.

Material Characterizations and Contact Angle Measurement. The family of 1-D C-curved nanoarches was characterized by field emission scanning electron microscopy (FESEM) on a JEOL JSM-6700F operating at 5 kV, by transmission electron microscopy and selected area electron diffraction (TEM/SAED) on a JEOL JEM-2010F operating at 200 kV, and by X-ray photoemission spectroscopy on a KRATOS AXIS Hsi with Al Kα radiation. Contact angle measurements made use of a First Ten Ångstroms FTA125 contact angle analyzer followed by curve fitting of the optical images obtained.

Supporting Information Available: Preparation and characterization of the precursor SnO_2 nanoparticles, additional XPS and FESEM data. This material is available free of charge *via* the Internet at http://pubs.acs.org.

REFERENCES AND NOTES

1. Park, M. S.; Wang, G. X.; Kang, Y. M.; Wexler, D.; Dou, S. X.; Liu, H. K. Preparation and Electrochemical Properties of SnO_2 Nanowires for Application in Lithium-Ion Batteries. *Angew. Chem., Int. Ed.* **2007**, *46*, 750.
2. Li, R. Y.; Sun, X. C.; Zhou, X. R.; Cai, M.; Sun, X. L. Aligned Heterostructures of Single-Crystalline Tin Nanowires Encapsulated in Amorphous Carbon Nanotubes. *J. Phys. Chem. C* **2007**, *111*, 9130.
3. Jankovic, L.; Gournis, D.; Trikalitis, P. N.; Arfaoui, I.; Cren, T.; Rudolf, P.; Sage, M. H.; Palstra, T. T. M.; Kooi, B.; De Hosson, J.; Karakassides, M. A.; Dimos, K.; Moukarika, A.; Bakas, T. Carbon Nanotubes Encapsulating Superconducting Single-Crystalline Tin Nanowires. *Nano Lett.* **2006**, *6*, 1131.
4. Law, M.; Greene, L. E.; Johnson, J. C.; Saykally, R.; Yang, P. D. Nanowire Dye-Sensitized Solar Cells. *Nat. Mater.* **2005**, *4*, 455.
5. Huang, L.; Lau, S. P.; Yang, H. Y.; Leong, E. S. P.; Yu, S. F.; Prawer, S. Stable Superhydrophobic Surface *via* Carbon Nanotubes Coated with a ZnO Thin Film. *J. Phys. Chem. B* **2005**, *109*, 7746.
6. Ge, S. P.; Jiang, K. L.; Lu, X. X.; Chen, Y. F.; Wang, R. M.; Fan, S. S. Orientation-Controlled Growth of Single-Crystal Silicon-Nanowire Arrays. *Adv. Mater.* **2005**, *17*, 56.
7. Bajpai, V.; Dai, L. M.; Ohashi, T. Large-Scale Synthesis of Perpendicularly Aligned Helical Carbon Nanotubes. *J. Am. Chem. Soc.* **2004**, *126*, 5070.
8. Sun, T.; Wang, G. J.; Liu, H.; Feng, L.; Jiang, L.; Zhu, D. B. Control over the Wettability of an Aligned Carbon Nanotube Film. *J. Am. Chem. Soc.* **2003**, *125*, 14996.
9. Lau, K. K. S.; Bico, J.; Teo, K. B. K.; Chhowalla, M.; Amaratunga, G. A. J.; Milne, W. I.; McKinley, G. H.; Gleason, K. K. Superhydrophobic Carbon Nanotube Forests. *Nano Lett.* **2003**, *3*, 1701.
10. Wang, Y.; Lee, J. Y. One-Step, Confined Growth of Bimetallic Tin−Antimony Nanorods in Carbon Nanotubes Grown *In Situ* for Reversible Li^+ Ion Storage. *Angew. Chem., Int. Ed.* **2006**, *45*, 7039.
11. Wang, Y. L.; Jiang, X. C.; Xia, Y. N. A Solution-Phase, Precursor Route to Polycrystalline SnO_2 Nanowires That Can Be Used for Gas Sensing under Ambient Conditions. *J. Am. Chem. Soc.* **2003**, *125*, 16176.
12. Liu, F.; Lee, J. Y.; Zhou, W. J. Multisegment PtRu Nanorods: Electrocatalysts with Adjustable Bimetallic Pair Sites. *Adv. Funct. Mater.* **2005**, *15*, 1459.
13. Liu, H.; Zhai, J.; Jiang, L. Wetting and Anti-wetting on Aligned Carbon Nanotube Films. *Soft Matter* **2006**, *2*, 811.
14. Deng, D.; Lee, J. Y. One-Step Synthesis of Polycrystalline Carbon Nanofibers with Periodic Dome-Shaped Interiors and Their Reversible Lithium-Ion Storage Properties. *Chem. Mater.* **2007**, *19*, 4198.
15. Gothard, N.; Daraio, C.; Gaillard, J.; Zidan, R.; Jin, S.; Rao, A. M. Controlled Growth of Y-Junction Nanotubes Using Ti-Doped Vapor Catalyst. *Nano Lett.* **2004**, *4*, 213.
16. Zhang, G. Y.; Jiang, X.; Wang, E. G. Tubular Graphite Cones. *Science* **2003**, *300*, 472.
17. Li, D. C.; Dai, L. M.; Huang, S. M.; Mau, A. W. H.; Wang, Z. L. Structure and Growth of Aligned Carbon Nanotube Films by Pyrolysis. *Chem. Phys. Lett.* **2000**, *316*, 349.
18. Li, J.; Tang, S. B.; Lu, L.; Zeng, H. C. Preparation of Nanocomposites of Metals, Metal Oxides, and Carbon Nanotubes *via* Self-Assembly. *J. Am. Chem. Soc.* **2007**, *129*, 9401.
19. Patzke, G. R.; Krumeich, F.; Nesper, R. Oxidic Nanotubes and Nanorods—Anisotropic Modules for a Future Nanotechnology. *Angew. Chem., Int. Ed.* **2002**, *41*, 2446.
20. Li, J.; Papadopoulos, C.; Xu, J. Nanoelectronics: Growing Y-Junction Carbon Nanotubes. *Nature* **1999**, *402*, 253.
21. Wei, B. Q.; Vajtai, R.; Ajayan, P. M. Sequence Growth of Carbon Fibers and Nanotube Networks by CVD Process. *Carbon* **2003**, *41*, 185.
22. Blossey, R. Self-Cleaning Surfaces—Virtual Realities. *Nat. Mater.* **2003**, *2*, 301.
23. Baughman, R. H.; Zakhidov, A. A.; de Heer, W. A. Carbon Nanotubes—The Route toward Applications. *Science* **2002**, *297*, 787.
24. Yang, L. L.; Zhao, Q. X.; Willander, M.; Yang, J. H. Effective Way to Control the Size of Well-Aligned ZnO Nanorod Arrays with Two-Step Chemical Bath Deposition. *J. Cryst. Growth* **2009**, *311*, 1046.
25. Wang, D. A.; Liu, Y.; Yu, B.; Zhou, F.; Liu, W. M. TiO_2 Nanotubes with Tunable Morphology, Diameter, and Length: Synthesis and Photo-Electrical/Catalytic Performance. *Chem. Mater.* **2009**, *21*, 1198.
26. Lafuma, A.; Quere, D. Superhydrophobic States. *Nat. Mater.* **2003**, *2*, 457.
27. Lee, K. T.; Jung, Y. S.; Oh, S. M. Synthesis of Tin-Encapsulated Spherical Hollow Carbon for Anode Material in Lithium Secondary Batteries. *J. Am. Chem. Soc.* **2003**, *125*, 5652.
28. Deng, D.; Lee, J. Y. Reversible Storage of Lithium in a Rambutan-like Tin−Carbon Electrode. *Angew. Chem., Int. Ed.* **2009**, *48*, 1660.
29. Huh, M. Y.; Kim, S. H.; Ahn, J. P.; Park, J. K.; Kim, B. K. Oxidation of Nanophase Tin Particles. *Nanostruct. Mater.* **1999**, *11*, 211.
30. Deng, D.; Lee, J. Y. Hollow Core−Shell Mesospheres of Crystalline SnO_2 Nanoparticle Aggregates for High Capacity Li^+ Ion Storage. *Chem. Mater.* **2008**, *20*, 1841.